

# Self-Assembly through Hydrogen Bonding: Peripheral Crowding—A New Strategy for the Preparation of Stable Supramolecular Aggregates Based on Parallel, Connected $\text{CA}_3\cdot\text{M}_3$ Rosettes

John P. Mathias, Eric E. Simanek, and George M. Whitesides\*

Contribution from the Department of Chemistry, Harvard University, Cambridge, Massachusetts 02138

Received September 29, 1993. Revised Manuscript Received February 27, 1994\*

**Abstract:** The self-assembly of two new types of stable hydrogen-bonded supramolecular aggregates—bisrosettes—that are based on parallel, connected  $\text{CA}_3\cdot\text{M}_3$  rosettes is reported. The minimization of intermolecular steric hindrance—peripheral crowding within the aggregate—is proposed as the structural feature responsible for selecting the cyclic  $\text{CA}_3\cdot\text{M}_3$  rosette over competing linear hydrogen-bonded networks available to the precursors. One series of aggregates— $3\text{bis}(\text{M})_2\cdot 6(\text{CA})$ —is composed of 3 equiv of a bulky bismelamine— $\text{bis}(\text{M})_2$ —and 6 equiv of a bulky isocyanurate (CA). The second series of aggregates— $3\text{bis}(\text{CA})_2\cdot 6(\text{M})$ —is composed of 3 equiv of a bisisocyanurate— $\text{bis}(\text{CA})_2$ —and 6 equiv of a melamine (M) bearing two bulky substituents. The nine particles in these aggregates are stabilized by 36 hydrogen bonds in two connected  $\text{CA}_3\cdot\text{M}_3$  rosettes. Each aggregate has been characterized by  $^1\text{H}$  NMR spectroscopy, gel permeation chromatography, and vapor pressure osmometry. Correlations between the size of the substituents and the preorganization of the precursors and the stability of the aggregates derived from them are discussed. Observations from  $^1\text{H}$  NMR spectroscopy and gel permeation chromatography indicate that aggregates comprising two connected  $\text{CA}_3\cdot\text{M}_3$  rosettes are more stable than those stabilized by a single  $\text{CA}_3\cdot\text{M}_3$  rosette, for similar extents of peripheral crowding in the rosettes.

## Introduction

This paper describes a strategy for the preparation of *stable* hydrogen-bonded self-assembling aggregates in which steric hindrance is used to *select* for the formation of one particular network of hydrogen bonds over many alternatives. The motif we wish to favor is the cyclic  $\text{CA}_3\cdot\text{M}_3$  “rosette” comprising three melamines (M) and three isocyanurates (CA) (Scheme 1).<sup>1–4</sup> Two additional cyclic hydrogen-bonded motifs have recently been demonstrated as the basis for supramolecular aggregates.<sup>5,6</sup> *Peripheral crowding* is the strategy we utilize here for assisting/directing the assembly of supermolecular aggregates based on the  $\text{CA}_3\cdot\text{M}_3$  rosette.<sup>7</sup>

In previous publications, we have described the self-assembly of hydrogen-bonded supramolecular aggregates in which a “hub and spoke” architecture was used to preorganize the melamine and isocyanurate components for the formation of stable  $\text{CA}_3\cdot\text{M}_3$  rosettes (Figure 1; *neohex*(CA) = *neohexylisocyanurate*).<sup>2,8,9</sup> Intermolecular steric hindrance between substituents in the hydrogen-bonded network can also be used to select the cyclic  $\text{CA}_3\cdot\text{M}_3$  “rosette” in preference to competing linear motifs, in both the solid and solution states (Scheme 1).<sup>7</sup> The presence of large substituents on barbitol (**1**) and *N,N'*-bis(4-*tert*-butyl-

phenyl)melamine (**2**) force these molecules to associate using the hydrogen-bonded network that places these groups far apart. This criterion is satisfied by the self-assembly of the  $\text{CA}_3\cdot\text{M}_3$  “rosette” (**3**) (Scheme 1). The crystal structure of the rosette (**3**) formed on crystallization from a solution of equimolar portions of **1** and **2** in toluene/isopropyl alcohol (1:1, v/v) is shown in Figure 2.<sup>10</sup> Although this aggregate displays a surprisingly high degree of stability in solution (considering that six particles are stabilized in a single aggregate by only 18 hydrogen bonds), it is the least stable supramolecular aggregate comprising melamines and isocyanurates that we have characterized to date.<sup>11</sup>

Our objective in this study was to develop the principle of peripheral crowding observed in the solid state into a general strategy for the self-assembly of *stable* hydrogen-bonded aggregates in solution. Our strategy was to assemble a new series of aggregates—bisrosettes—based on two parallel, connected  $\text{CA}_3\cdot\text{M}_3$  rosettes. The qualitative basis for this approach was to increase the difference between the favorable *enthalpy* of association (a value correlated with the number of hydrogen bond stabilizing the aggregate) and the unfavorable entropy of association (related to the number of particles associated in the final aggregate).<sup>12</sup> The progression from supramolecular aggregates based on single  $\text{CA}_3\cdot\text{M}_3$  rosettes to aggregates comprising two connected  $\text{CA}_3\cdot\text{M}_3$  rosettes is illustrated in Scheme 2. The “bisrosette” **6** comprises 3 equiv of the bismelamine **4** and 6 equiv of the bulky isocyanurate **5**. The nine particles in **6** are stabilized by 36 hydrogen bonds. By contrast, the six particles in **3** were stabilized by only 18 hydrogen bonds. We predicted, therefore, that **6** would be more stable than **3**.

\* Abstract published in *Advance ACS Abstracts*, April 1, 1994.

(1) Whitesides, G. M.; Mathias, J. P.; Seto, C. T. *Science* **1991**, 254, 1312–1319.

(2) Seto, C. T.; Whitesides, G. M. *J. Am. Chem. Soc.* **1993**, 115, 905–916.

(3) Seto, C. T.; Mathias, J. P.; Whitesides, G. M. *J. Am. Chem. Soc.* **1993**, 115, 1321–1329.

(4) Seto, C. T.; Whitesides, G. M. *J. Am. Chem. Soc.* **1993**, 115, 1330–1340.

(5) Zimmerman, S. C.; Duerr, B. F. *J. Org. Chem.* **1992**, 57, 2215–2217.

(6) Geib, S. J.; Vicent, C.; Fan, E.; Hamilton, A. D. *Angew. Chem. Int. Ed. Engl.* **1993**, 32, 119–121.

(7) Mathias, J. P.; Simanek, E. E.; Zerkowski, J. A.; Seto, C. T.; Whitesides, G. M. *J. Am. Chem. Soc.* Submitted for publication.

(8) Mathias, J. P.; Seto, C. T.; Simanek, E. E.; Whitesides, G. M. *J. Am. Chem. Soc.* **1994**, 116, 1725–1736.

(9) Mathias, J. P.; Simanek, E. E.; Seto, C. T.; Whitesides, G. M. *Angew. Chem. Int. Ed. Engl.* In press.

(10) Zerkowski, J. A.; Seto, C. T.; Whitesides, G. M. *J. Am. Chem. Soc.* **1992**, 114, 5473–5475.

(11)  $^1\text{H}$  NMR exchange experiments indicate that the ground-state free energy for the  $\text{CA}_3\cdot\text{M}_3$  rosette **3** is greater than 3 kcal/mol higher (it is less stable) than that for the supramolecular aggregate  $\text{hub}(\text{M})_3\cdot 3\text{barbitol}$ —an analog of  $\text{hub}(\text{M})_3\cdot 3\text{neohex}(\text{CA})$  (Figure 1).

(12) The correlation of the stability of an aggregate to the number of hydrogen bonds stabilizing it and the number of particles associated has been presented on a qualitative level in ref 8.

Scheme 1

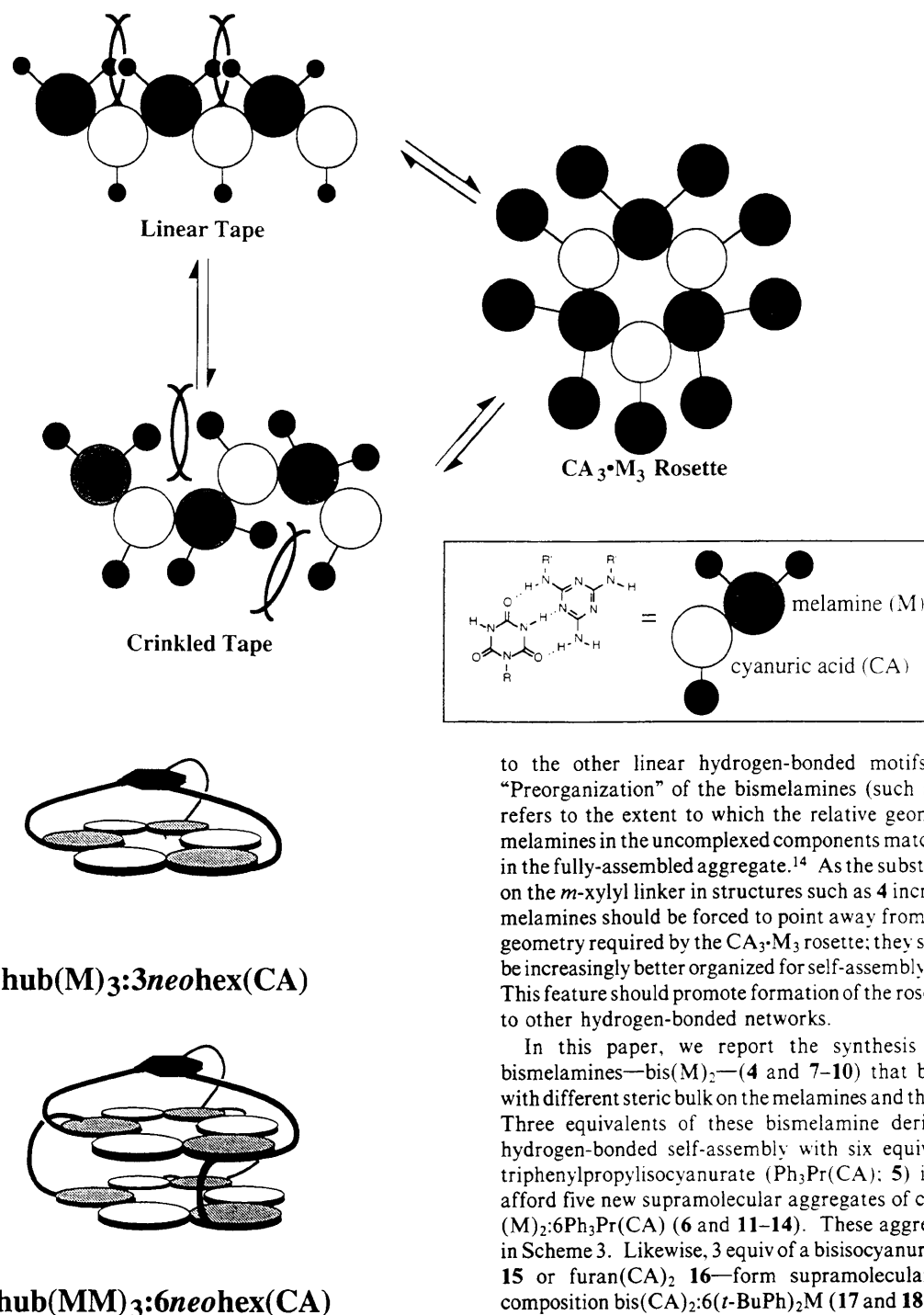


**Figure 1.** Schematic representations of two types of supramolecular aggregates based on  $CA_3 \cdot M_3$  rosettes that preorganized for self-assembly through a "hub and spoke" architecture.

In addition to determining whether the progression from single rosettes to bisrosettes is accompanied by an increase in stability, we also hoped to (i) examine the effects of changes in the steric bulk and preorganization of the components on the formation and stability of the supramolecular aggregates and (ii) compare and contrast the stability and structural integrity of aggregates obtained by peripheral crowding to those we have obtained using covalent preorganization to assist self-assembly. We expected that the potential for intermolecular steric hindrance between neighbors would increase as the size of the peripheral substituents increased, and predicted that the formation of the cyclic  $CA_3 \cdot M_3$  rosette would, therefore, become increasingly favorable, relative

to the other linear hydrogen-bonded motifs (Scheme 1).<sup>13</sup> "Preorganization" of the bismelamines (such as **4**, Scheme 2) refers to the extent to which the relative geometry of the two melamines in the uncomplexed components match their geometry in the fully-assembled aggregate.<sup>14</sup> As the substituent (e.g., *Pr*) on the *m*-xylyl linker in structures such as **4** increases in size, the melamines should be forced to point away from the linker in the geometry required by the  $CA_3 \cdot M_3$  rosette; they should, therefore, be increasingly better organized for self-assembly of the aggregate. This feature should promote formation of the rosette in preference to other hydrogen-bonded networks.

In this paper, we report the synthesis of a series of bismelamines—bis(M)<sub>2</sub>—(**4** and **7–10**) that bear substituents with different steric bulk on the melamines and the *m*-xylyl linkers. Three equivalents of these bismelamine derivatives undergo hydrogen-bonded self-assembly with six equivalents of 3,3,3-triphenylpropylisocyanurate (Ph<sub>3</sub>Pr(CA); **5**) in chloroform to afford five new supramolecular aggregates of composition 3bis(M)<sub>2</sub>:6Ph<sub>3</sub>Pr(CA) (**6** and **11–14**). These aggregates are shown in Scheme 3. Likewise, 3 equiv of a bisisocyanurate—benz(CA)<sub>2</sub> **15** or furan(CA)<sub>2</sub> **16**—form supramolecular aggregates of composition bis(CA)<sub>2</sub>:6(*t*-BuPh)<sub>2</sub>M (**17** and **18**, respectively) on mixing with 6 equiv of *N,N'*-bis(4-*tert*-butylphenyl)melamine—(*t*-BuPh)<sub>2</sub>M—(**2**). These aggregates are shown in Scheme 4.

## Results

**Design and Synthesis of the Components.** Two strategies have been used for the synthesis of the bismelamine derivatives **4** and **7–10**. The stepwise synthesis of the bismelamine **4** is shown in Scheme 5. The other symmetrical bismelamine derivatives **7–10** were synthesized using the more direct strategy shown for **7** in Scheme 6. The syntheses of **2**,<sup>2,5,8</sup> **15**,<sup>3</sup> and **16**<sup>3</sup> have been reported previously.

The structures of the bismelamines are easily modified by synthesis. The feature has allowed specific hypotheses relating

(13) Zerkowski, J. A.; Seto, C. T.; Wierda, D. A.; Whitesides, G. M. *J. Am. Chem. Soc.* **1993**, In press.

(14) Cram, D. J. *Angew. Chem., Int. Ed. Engl.* **1986**, *25*, 1039–1057.

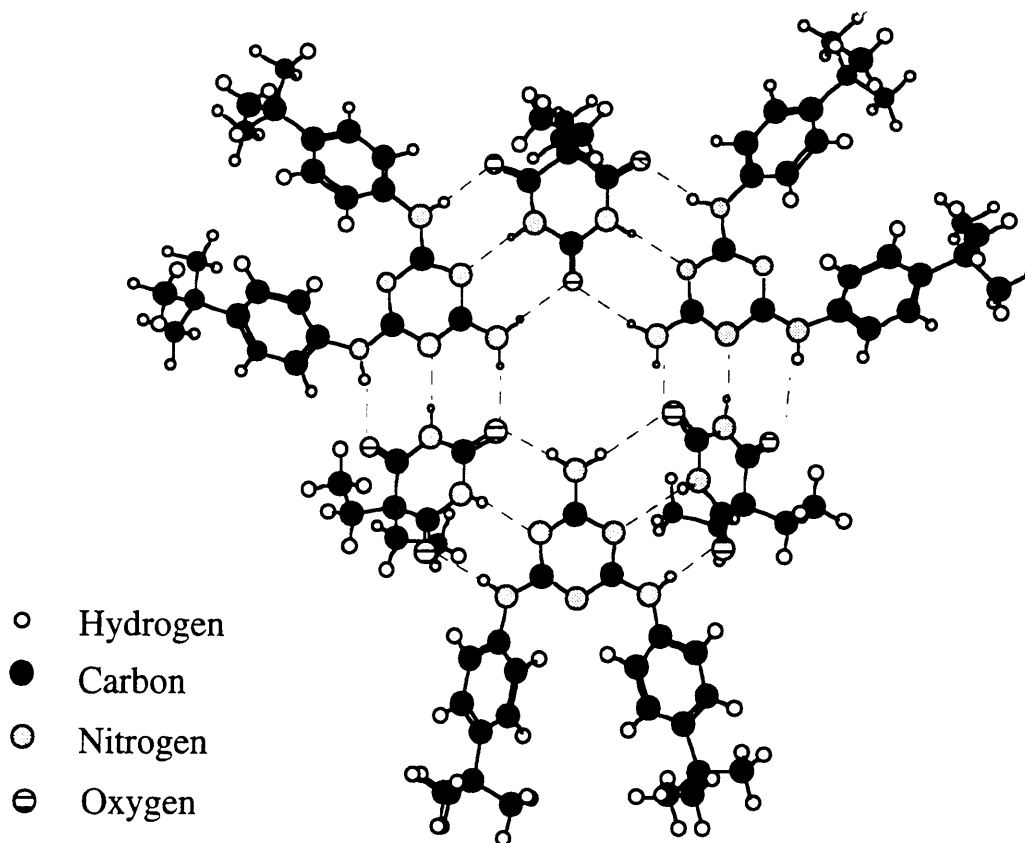


**Figure 2.** X-ray crystal structure of the  $CA_3 \cdot M_3$  rosette formed on mixing equimolar portions of barbital and  $N,N'$ -bis(4-*tert*-butylphenyl)melamine in a solution of toluene/isopropyl alcohol (1:1 v/v).

to the steric bulk of the substituents on the melamines and preorganization of the components to be tested. Linking two melamines (as in **4** and **7–10**) does not constrain them to lie over each other (eclipsed) or away from each other (staggered); they are free to rotate freely relative to each other. This feature creates the potential for conformational isomerism in the self-assembled aggregates.

The bisisocyanurates **15** and **16** are more difficult to synthesize in structurally modified forms than are the bismelamines. These compounds also exhibit low solubilities in chloroform (<0.1 mM). Using bisisocyanurates as the basis of a strategy for the self-assembly of aggregates is, therefore, less practical than using bismelamines. Both **15** or **16** bear isopropyl groups that may contribute to the self-assembly of  $CA_3 \cdot M_3$  rosettes by peripheral crowding.

**Design and Preparation of Supramolecular Aggregates.** We have developed two closely related strategies to prepare self-assembled aggregates that are based on peripheral crowding and are stabilized by two parallel, connected  $CA_3 \cdot M_3$  rosettes. In the first approach, 3 equiv of the bismelamines **4** and **7–10** were mixed with 6 equiv of the monomeric isocyanurate **5** in chloroform to afford aggregates of composition  $3bis(M)_2:6Ph_3Pr(CA)$  (Scheme 3). Although the solubility of the uncomplexed bismelamine and isocyanurate components in chloroform is low (<2 mM in all cases), the supramolecular aggregates **6** and **11–14** were obtained as homogeneous solutions after sonicating the components (~15 s) and heating to reflux (~20 s).<sup>15</sup> In the second approach, 3 equiv of the bisisocyanurates **15** or **16** were mixed with 6 equiv of the melamine **2** in MeOH/ $CHCl_3$  (1:9 v/v) to give aggregates of composition  $3bis(CA)_2:6(t-BuPh)_2M$  (Scheme 4). The suspension was heated to reflux (~15 s) to afford a homogeneous solution. Removal of the solvent in vacuo gave the aggregates **17** and **18**, respectively, as white solids that were soluble in chloroform alone. Although the solubilities of the aggregates based on bismelamines **6** and **11–14** in chloroform were higher than those based on the bisisocyanurates **17** and **18**,

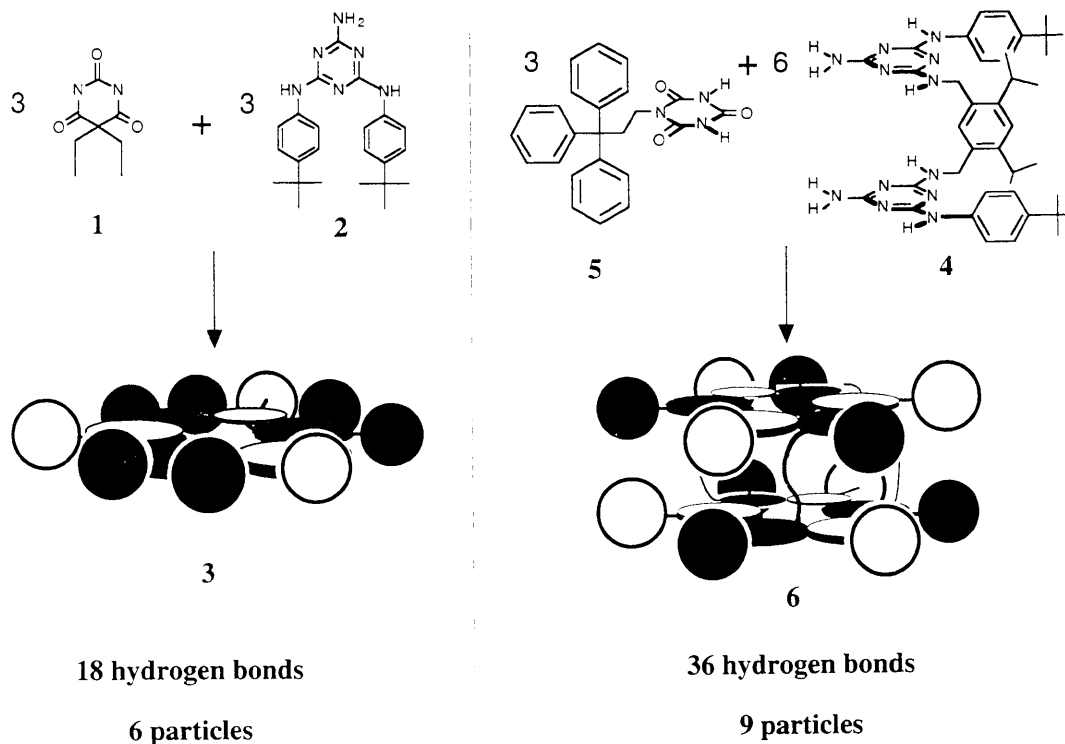
both of these new types of aggregates exhibited the lowest solubilities of any aggregates that we have studied to date (<15 mM in chloroform in all cases). The solubility of the rosette **3** (Scheme 2) in chloroform was >80 mM.

**Characterization of the Supramolecular Aggregates.** We have described previously the characterization of hydrogen-bonded aggregates using  $^1H/^{13}C$  NMR spectroscopy (local structure), gel permeation chromatography (molecular size, dispersity, and relative stability), and vapor pressure osmometry (molecular weight and concentration-dependent behavior in solution). Data obtained from these three techniques are presented for the aggregates **6** (Scheme 3) and **18** (Scheme 4) to illustrate the structural features, size, and stability of these aggregates. The emphasis of this section, however, is to compare and contrast the behavior/structure of these new “bisrosettes” aggregates with those of single rosettes<sup>7</sup> and aggregates based on connected  $CA_3 \cdot M_3$  rosettes obtained using covalent preorganization to direct self-assembly.<sup>2,3,8</sup>

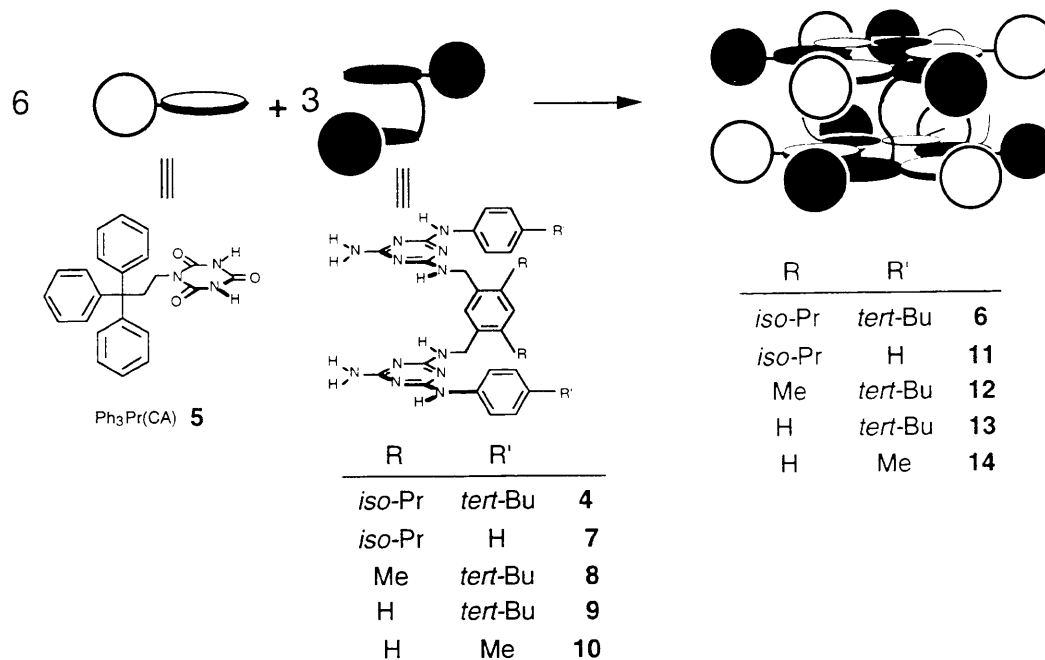
**(i)  $^1H$  NMR Spectroscopy.** Figure 3 shows the  $^1H$  NMR spectra of the aggregates **6** and **18**. These spectra can be assigned to the structures shown for **6** and **18** using COSY, NOESY, and 1-D NOE measurements (Figure 4). Resonances in the spectra of the uncomplexed components **4** and **16** in  $CDCl_3$  and  $DMSO-d_6$  are significantly less well-defined than those for the aggregates, as a consequence of self-association and hindered rotation.

Both **6** and **18** exhibit two resonances for the isocyanurate protons,  $H^{1,2}$  (see Figure 4 for labeling), with chemical shifts between  $\delta$  14 and 16 ppm in  $CDCl_3$  (Figure 3). The low-field chemical shifts of these signals are consistent with the involvement of the isocyanurate protons in a strong hydrogen-bonded network.<sup>16</sup> The observation of two resonances for the isocyanurate protons in **6** suggests that the two parallel  $CA_3 \cdot M_3$  rosettes in this aggregate are related by symmetry and that rotation of the isocyanurates around their 2-fold axes is slow on the NMR time scale. The unsymmetrical substitution of the melamines in **6** imparts two different environments to the isocyanurate protons,

**Scheme 2.** Strategy for Increasing the Stability of Aggregates Obtained by Peripheral Crowding Involves the Progression from Structures Comprising a Single  $CA_3 \cdot M_3$  Rosette (3) to "Bisrosettes" Such As 6 in Which the Two Rosettes Are Connected through Covalent Linkers between Melamine or Isocyanurate (Not Shown) Derivatives



**Scheme 3.** Self-Assembly of Supramolecular Aggregates of Composition  $3bis(M)_2:6Ph_3Pr(CA)$  6 and 11–14



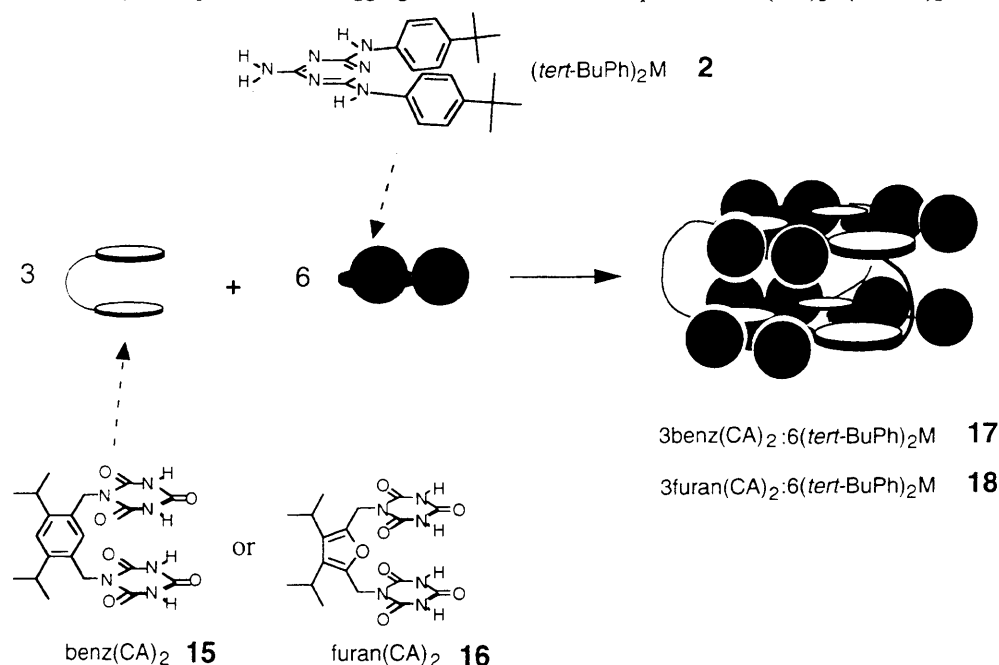
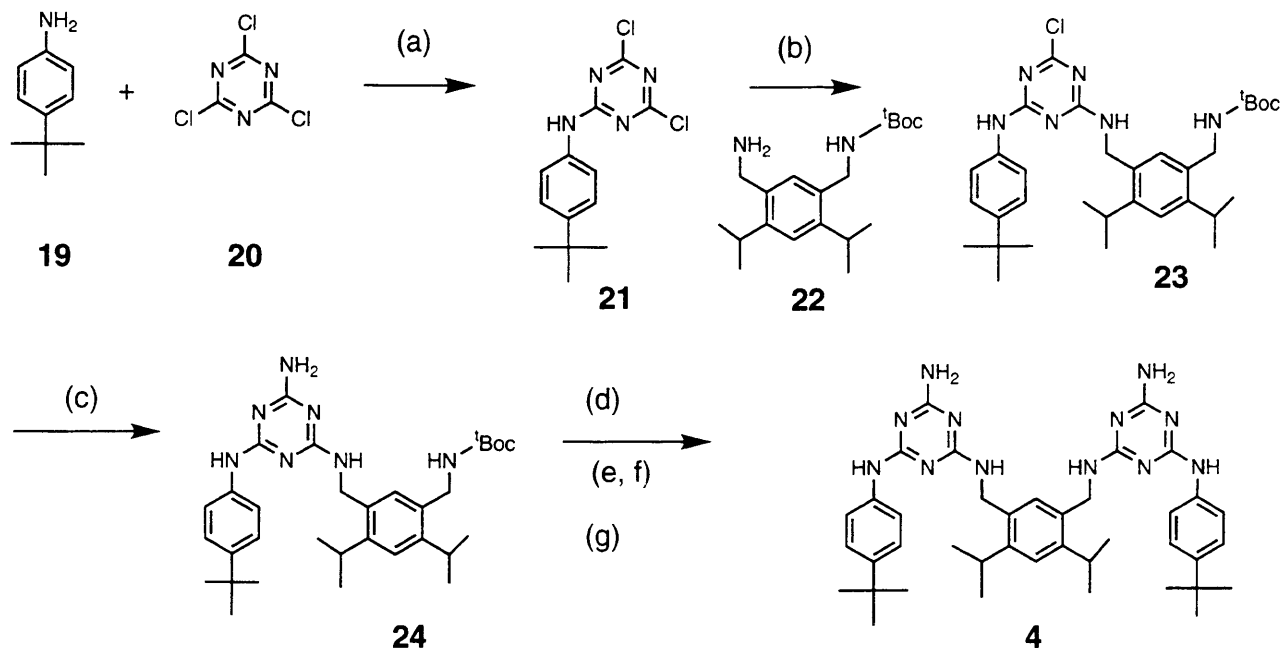
such that  $H^1 \neq H^2$  in each  $CA_3 \cdot M_3$  rosette. One isocyanurate proton ( $H^1$ ) is adjacent to the *m*-xylyl group and the second isocyanurate proton ( $H^2$ ) is adjacent to the *p*-*tert*-butylphenyl substituent (Figure 4). Figure 5 shows two possible conformations that would allow the adjacent rosettes to be related by at least 2-fold symmetry. These conformations are (i) an eclipsed conformation, in which melamines and isocyanurates in adjacent rosettes lie in registry with each other—the two rosettes would then be related by a mirror plane of symmetry; top = bottom—and (ii) the staggered conformation, in which the melamines in one rosette lie over isocyanurates in the connected rosette and visa versa—the two rosettes would then be related by a rotation of the

aggregate by  $180^\circ$  about an axis running through the atoms k and l in the linker (labels shown in Figure 4). The staggered conformation is obtained from the eclipsed by a rotation of  $180^\circ$  about one of the melamineNH-xylyl bonds.<sup>17</sup>

The observation of two resonances for the isocyanurate protons  $H^{1,2}$  in 18 (resonances for all other protons in the  $CA_3 \cdot M_3$  rosette are also doubled) suggests the two rosettes lie staggered relative to each other, with the melamines over the cyanurates, rather

(15) The formation of these aggregates as homogeneous solutions in chloroform from their insoluble precursors is a common feature in these systems.

(16) These protons appear at  $\delta$  11.2 in the free isocyanurate dissolved in DMSO- $d_6$ .

**Scheme 4.** Self-Assembly of Supramolecular Aggregates **17** and **18** of Composition  $3\text{bis}(\text{CA})_2:6(t\text{-BuPh})_2\text{M}$ **Scheme 5.** Synthesis of the Bismelamine Derivative **4**

than directly in registry, with melamines over each other and a horizontal plane of symmetry. The staggered/tilted conformation of the parallel  $\text{CA}_3\cdot\text{M}_3$  rosettes in **18** suggests that there must be a driving force for the rings not to lie eclipsed. We suggest that the origin of this effect is to avoid steric crowding between the *tert*-butylphenyl groups in adjacent  $\text{CA}_3\cdot\text{M}_3$  rosettes. The tilting of the furanyl linker introduces an asymmetry to **18** that is similar to that observed for **6**. One isocyanurate proton ( $\text{H}^1$ ) lies away from the direction in which the linker is "tilting" and the second isocyanurate proton ( $\text{H}^2$ ) lies toward the direction in which the linker is "tilting" (Figure 4). The upper and lower  $(\text{CA})\cdot(\text{M})$

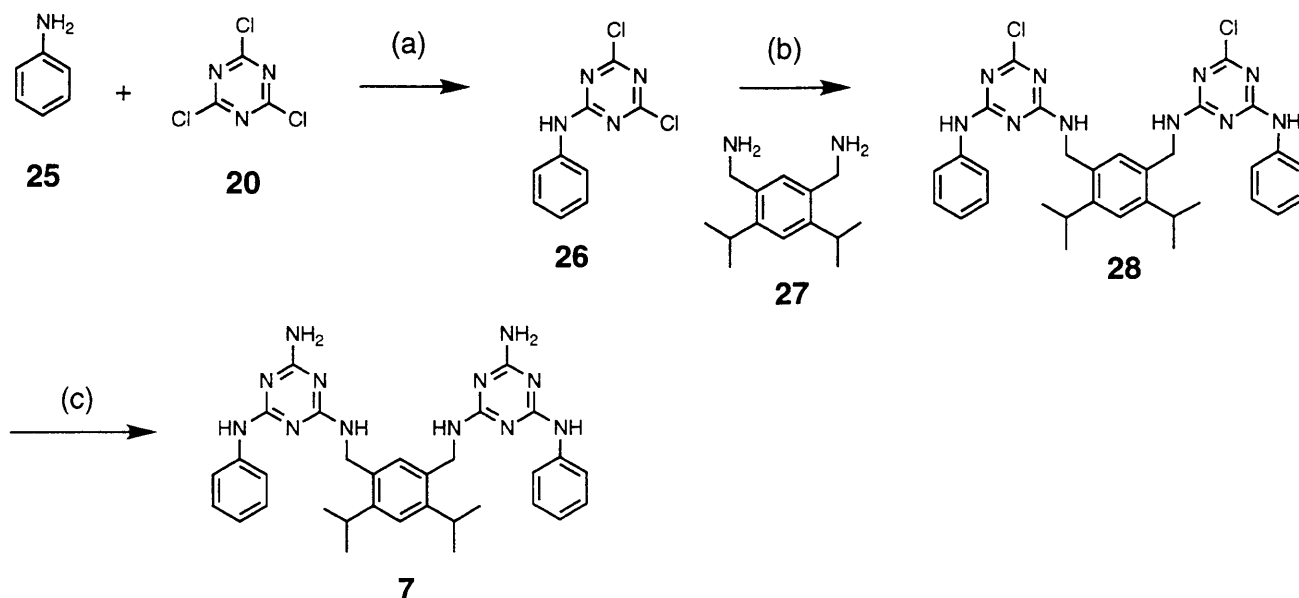
(17) We believe that the actual structure of **6** is, in fact, the staggered conformation shown in Scheme 2. This conformation reduces unfavorable steric crowding between the three triphenylpropyl and three *p*-*tert*-butylphenyl groups on the periphery of each adjacent  $\text{CA}_3\cdot\text{M}_3$  rosette by allowing them to interdigitate more effectively around the edge of the hydrogen-bonded network. The staggered conformation may also allow matching of the partial charges in the "stacked" heterocyclic isocyanurate and melamines.

units shown for **18** in Figure 4 are, therefore, related by a  $C_2$  axis of rotation. The observation of two distinct sets of resonances for **18** suggests that interconversion between the two enantiomers **18a** and **18b** (Figure 6) must be slow on the NMR time scale.

The appearance of two resonances for the furanyl protons  $\text{H}^5$  and  $\text{H}^5'$  of **18** is also compatible with a chiral aggregate. Two sets of the resonances ( $\text{H}^{6,7}$ ) for the isopropyl methyl groups are hidden by a large signal for the *p*-*tert*butylphenyl groups on the melamines.

Strong NOE interactions between protons confirm the geometry of the hydrogen-bonded  $\text{CA}_3\cdot\text{M}_3$  rosettes in **6** and **18**. These interactions are tabulated in Figure 4. There are no significant changes in chemical shift, line width/shape, relative proportions by integration, or number of resonances for either **6** or **18** as the temperature is decreased from 298 to 233 K.

$^1\text{H}$  NMR spectra from the titration of 2 equiv of the isocyanurate **5** into 1 equiv of the bismelamine **4** in  $\text{CDCl}_3$  are

**Scheme 6.** Synthesis of the Bismelamine Derivative **7**

also shown in Figure 3. At a stoichiometry of 1:2 for **4**:**5**, a single set of resonances is visible that can be assigned to the aggregate **6** (Figure 4). At stoichiometries less than 1:2 for **4**:**5**, resonances for the fully assembled aggregate **6** and the uncomplexed bismelamine **4** are visible. An additional set of resonances (–; Figure 3) can also be seen at this stoichiometry. The sharp nature of the additional resonances and the presence of two resonances around  $\delta$  15 ppm leads us to suggest that the origin of these signals may be an aggregate in which only a single  $\text{CA}_3\cdot\text{M}_3$  rosette has assembled.<sup>18</sup> This type of aggregate would be a direct analog of the rosettes formed between 3 equiv of bulky melamines and isocyanurates we have reported previously.<sup>7</sup>

The observation of separate sets of resonances for the complexed and uncomplexed states during the titration of **5** into **4** indicates that exchange between these states is slow on the time scale of NMR spectroscopy. This stability toward exchange contrasts with the instability of rosettes formed between monomeric melamines and barbiturates; in these cases, exchange between the assembled and uncomplexed states was rapid on the NMR time scale.<sup>7</sup> The progression from aggregates based on a single  $\text{CA}_3\cdot\text{M}_3$  rosette to those comprising two parallel, connected  $\text{CA}_3\cdot\text{M}_3$  rosettes is, therefore, accompanied by a decreased rate of dynamic exchange at 298 K.

Dilution of solutions of the aggregates in chloroform from 3 to 0.05 mM did not result in any dissociation of the aggregates, as judged by  $^1\text{H}$  NMR spectroscopy. We observed no change in the chemical shifts of the hydrogen-bonded protons on dilution. This feature again contrasts to the behavior observed for aggregates comprising a single  $\text{CA}_3\cdot\text{M}_3$  rosette.<sup>7</sup> In these cases, dilution of the aggregates in chloroform below 3.5 mM resulted in large upfield shifts of the hydrogen-bonded protons and suggested a reduction in the degree of hydrogen bonding as the concentration was decreased.

**(ii) Gel Permeation Chromatography.** Figure 7 shows traces for **6** and **18** from gel permeation chromatography (GPC) using chloroform or methylene chloride as the eluent. In each case, the aggregates give well-defined peaks by GPC. The relatively sharp leading edges (to shorter retention time) and moderate tailing exhibited by **6** and **18** contrast to observations made by GPC for aggregates such as **3** that are based on a single  $\text{CA}_3\cdot\text{M}_3$  rosette. The stability of **3** was too low for it to elute intact from the GPC column; no peaks were observed. We infer that **3** dissociated completely during the time required for analysis (7–9 min).<sup>19</sup>

(18) We do not usually see defined resonances in  $^1\text{H}$  NMR spectroscopy from “irregular” or more random H-bonded oligo/polymers.

The observation of well-defined peaks with retention times in the range 8–9 min for **6** and **18** is consistent with data obtained for other stable hydrogen-bonded aggregates we have described previously. These results for **6** and **18** are, therefore, another indication that the progression from aggregates stabilized by single  $\text{CA}_3\cdot\text{M}_3$  rosettes to aggregates stabilized by two connected  $\text{CA}_3\cdot\text{M}_3$  rosettes—whether the constitution is  $3(\text{CA})_2\cdot 6(\text{M})$  or  $3(\text{M})_2\cdot 6(\text{CA})$ —is accompanied by a substantial increase in stability. The peak shapes for **6** and **18** suggest that the stability of these aggregates is comparable to  $\text{hub}(\text{MM})_3\cdot 6\text{neohex}(\text{CA})^8$  and greater than  $\text{hub}(\text{M})_3\cdot 3\text{neohex}(\text{CA})^2$ . Traces for these aggregates are also shown in Figure 7 for comparison.

**(iii) Vapor Pressure Osmometry.** Molecular weights for **6** and **18** have been determined by vapor pressure osmometry in chloroform solution (Figure 8a). Plots of  $\Delta V/\text{concn}$  vs  $\text{concn}$  from which the molecular weights were obtained are illustrated in Figure 8b.<sup>20</sup> The data for **6** ( $\blacktriangle$ , solid line) display a modest positive slope. Those for **18** ( $\cdot$ , dashed line), however, display a negative slope.<sup>21</sup> The latter observation is consistent with concentration-dependent association of this aggregate.<sup>22</sup> Non-specific association of **18** would explain why the values obtained for the molecular weight of this aggregate in solution are consistently higher than the expected value.

**Aggregates Formed between Complementary Bismelamines and Bisocyanurates.** Mixing equimolar portions of the bisocyanurate **15** with the bismelamine **4** does not afford an aggregate in which 3 equiv of each component combine in two parallel  $\text{CA}_3\cdot\text{M}_3$  rosettes (Scheme 7). Although the mixture affords a homogeneous solution in chloroform,  $^1\text{H}$  NMR spectroscopy does not reveal the presence of a well-defined aggregate, such as **29**. Instead, the resonances are poorly defined, broad, and many. This feature is illustrated clearly by the many separate resonances observed for the isocyanurate protons shown in Figure 9a. The structural complexity evident from this portion of the  $^1\text{H}$  NMR spectrum of the aggregate is also seen in the remainder of the spectrum. The result of mixing **4** and **15** appears, therefore, to be an extended hydrogen-bonded structure containing many

(19) A discussion of the correlation between stability of an aggregate and its peak shape in GPC is presented in ref 8.

(20) VPO requires calibration against a standard of known molecular weight. The standard and the new aggregate of unknown weight are then related by  $\text{MW}_{\text{standard}} \lim_{c \rightarrow 0} [\Delta V/c_{\text{standard}}] = \text{MW}_{\text{aggregate}} \lim_{c \rightarrow 0} [\Delta V/c_{\text{aggregate}}]$ . The ratio  $\Delta V/c$  (in the limit as  $c \rightarrow 0$ ) is determined by VPO ( $c$  = concentration,  $\Delta V$  is proportional to the change in vapor pressure measured by VPO).

(21) An ideal solute would give a straight line with zero slope in a plot of  $\Delta V/\text{concn}$  vs  $\text{concn}$ .

(22) We have discussed this feature in refs 2 and 4.

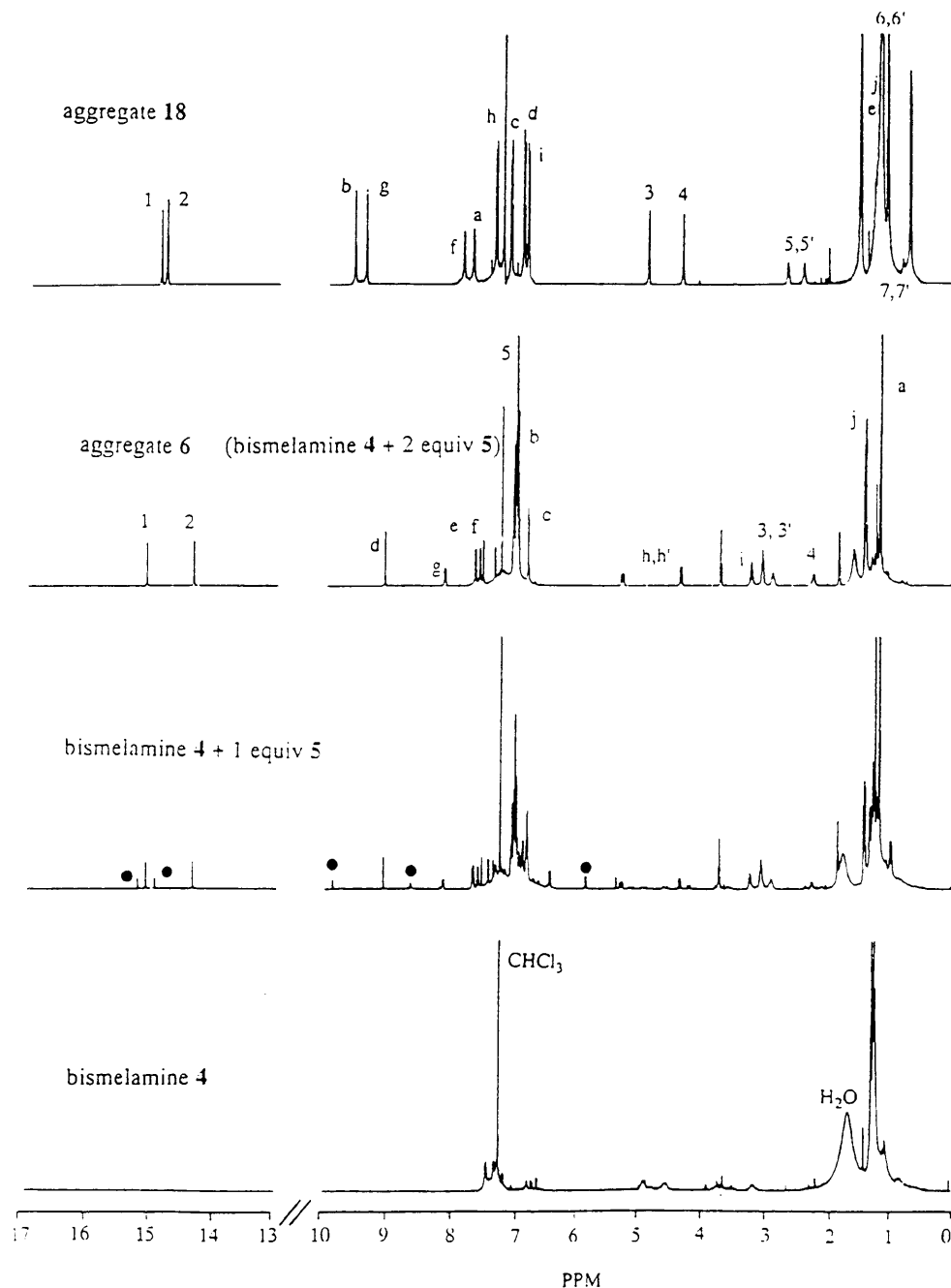


**Figure 3.**  $^1\text{H}$  NMR spectra of the supramolecular aggregates **6** and **18** ( $\text{CDCl}_3$ , 500 MHz). Annotations refer to Figure 4. The resonances indicated by  $\bullet$  are proposed to belong to a partly formed aggregate containing one rosette; see the text for discussion.

different structural subelements. One possibility may be a range of different "vernier-type" polymers, such as that represented by **30** (Scheme 7). The multiplicity in this spectrum is not an artifact of the kinetics of assembly: there is not change in the spectrum of the mixture on heating the solution at 45 °C for 7 days. We note that  $\text{benz}(\text{CA})_2$  **15** does form an aggregate (**17**; Scheme 4) of composition  $3\text{benz}(\text{CA})_2:6(t\text{-BuPh})_2\text{M}$  with the melamine **2**. The steric requirements for assembly of  $\text{CA}_3\text{-M}_3$  rosettes with **15** should, therefore, be satisfied by the bismelamine **4**. One explanation for the failure of **4** and **15** to yield a discrete aggregate may be the inability of the conformationally rigid bisisocyanurate to satisfy the staggered arrangement that we believe to be favored by the bismelamine **4** in the aggregates **6** and **11–14**.

**Aggregates Formed by Unsymmetrical Bismelamines.** Mixing 3 equiv of the unsymmetrical bismelamine **31** with 6 equiv of the isocyanurate **5** in chloroform does not afford a single aggregate (for example, **32**) in which the three melamines adopt the same "orientation" (Scheme 8). Instead, in this instance  $^1\text{H}$  NMR

spectroscopy reveals the presence of multiple resonances and suggests the formation of several different hydrogen-bonded states. There does not appear to be any preference for the bismelamine components to orient themselves in a discrete aggregate (**32**) with the *p*-*tert*-butylphenyl substituent in one  $\text{CA}_3\text{-M}$  rosette and the *neo*hexyl substituents in the other  $\text{CA}_3\text{-M}_3$  rosette. A mixture of the isomers **32** and **33**, however, could, in principle, generate many local environments for the isocyanurate protons. No change occurs in this spectrum on heating the solution at 50 °C for 5 days.

## Discussion

*Changing the steric bulk and preorganization of the components has a significant effect on the self-assembly of supramolecular aggregates based on peripheral crowding.* We have examined the effects of four different aspects of the structure of the uncomplexed components on the structural integrity and stability of supramolecular aggregates derived from them. They

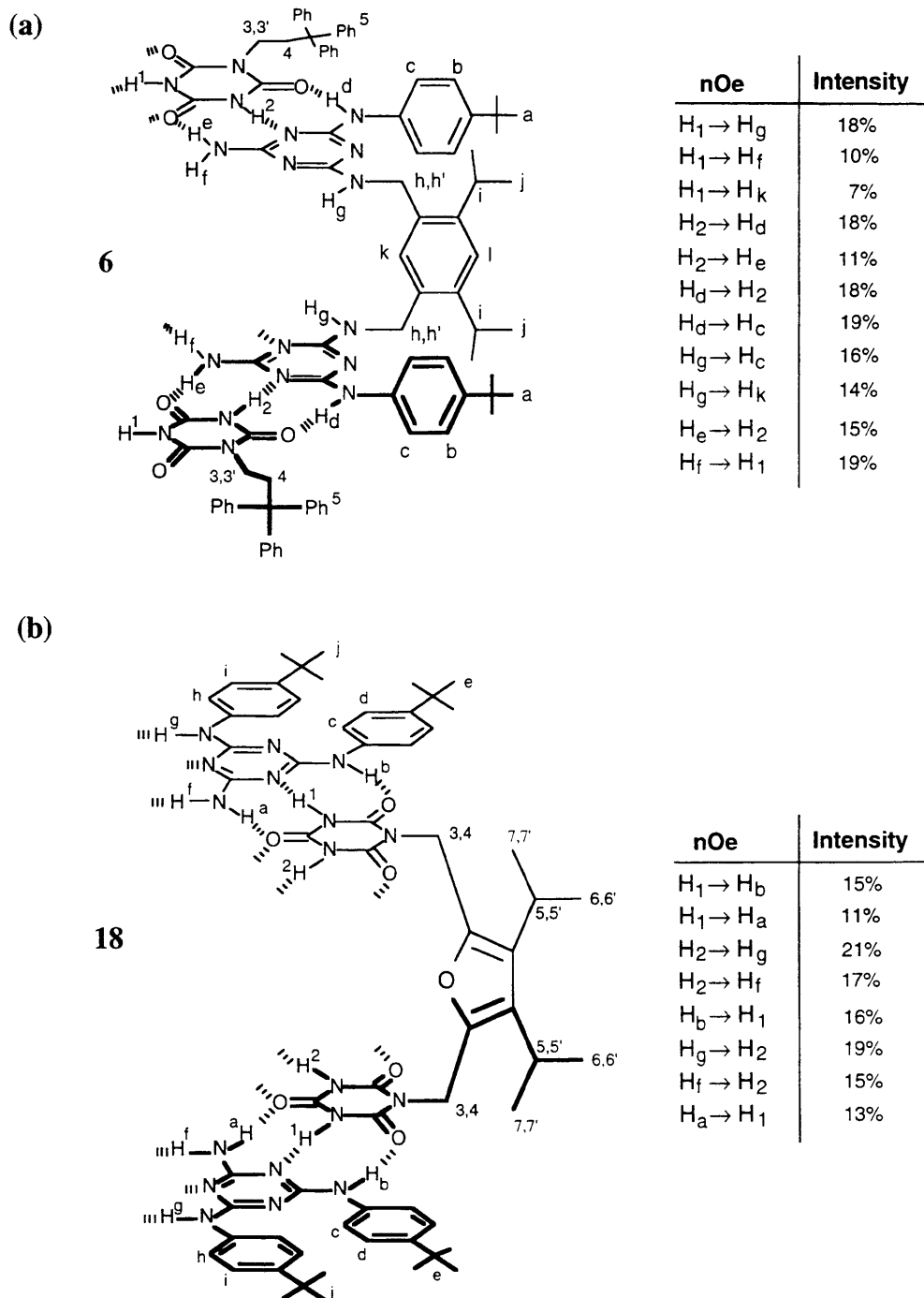


**Figure 4.** Assignment of resonances and selected NOE interactions in the  $^1\text{H}$  NMR spectra of the aggregates **6** (a) and **18** (b). Labels refer to the peaks shown in Figure 3. NOE interactions with intensities below 5% are not included.

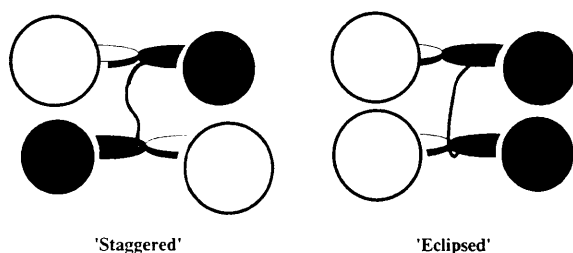


**Figure 5.** Schematic representation of two extreme conformations that are possible for aggregates based on bismelamine derivatives.

are the role of (i) the steric bulk of the substituent (the group R' in Table 1) on the melamines in aggregates based on bismelamines, (ii) the steric bulk of the isocyanurate or barbiturate in aggregates based on bismelamines, (iii) the preorganization of the melamines

in the bismelamines for assembly of the  $\text{CA}_3\cdot\text{M}_3$  rosette, *i.e.*, size of the group R in Table 1, and (iv) the steric bulk of the melamines in aggregates based on bisisocyanurates. These aspects will be discussed in turn.

The outcome of mixing 3 equiv of the bismelamines **4** and **7–10** with 6 equiv of the isocyanurates **5** or **34** or with the barbiturates **1** or **35** is illustrated in Table 1. Successful formation of a stable "bisrosette" aggregate (as judged by  $^1\text{H}$  NMR spectroscopy) is indicated by ++. Failure of the 3 equiv of the bismelamine to solubilize 6 equiv of the isocyanurate/barbiturate is denoted by -. The soluble portion obtained by filtering these suspensions did not contain any well-defined aggregates. Instead, the resonances in the  $^1\text{H}$  NMR spectra were poorly defined and broad. The marker + denotes the formation of an aggregate from which the original homogeneous solution exhibits slow, but significant, precipitation over time (>24 h).



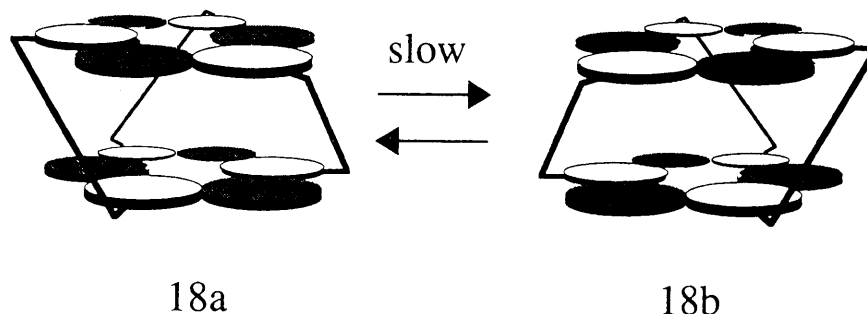


Figure 6. Interconversion of the two enantiomers **18a** and **18b** is slow on the NMR time scale.

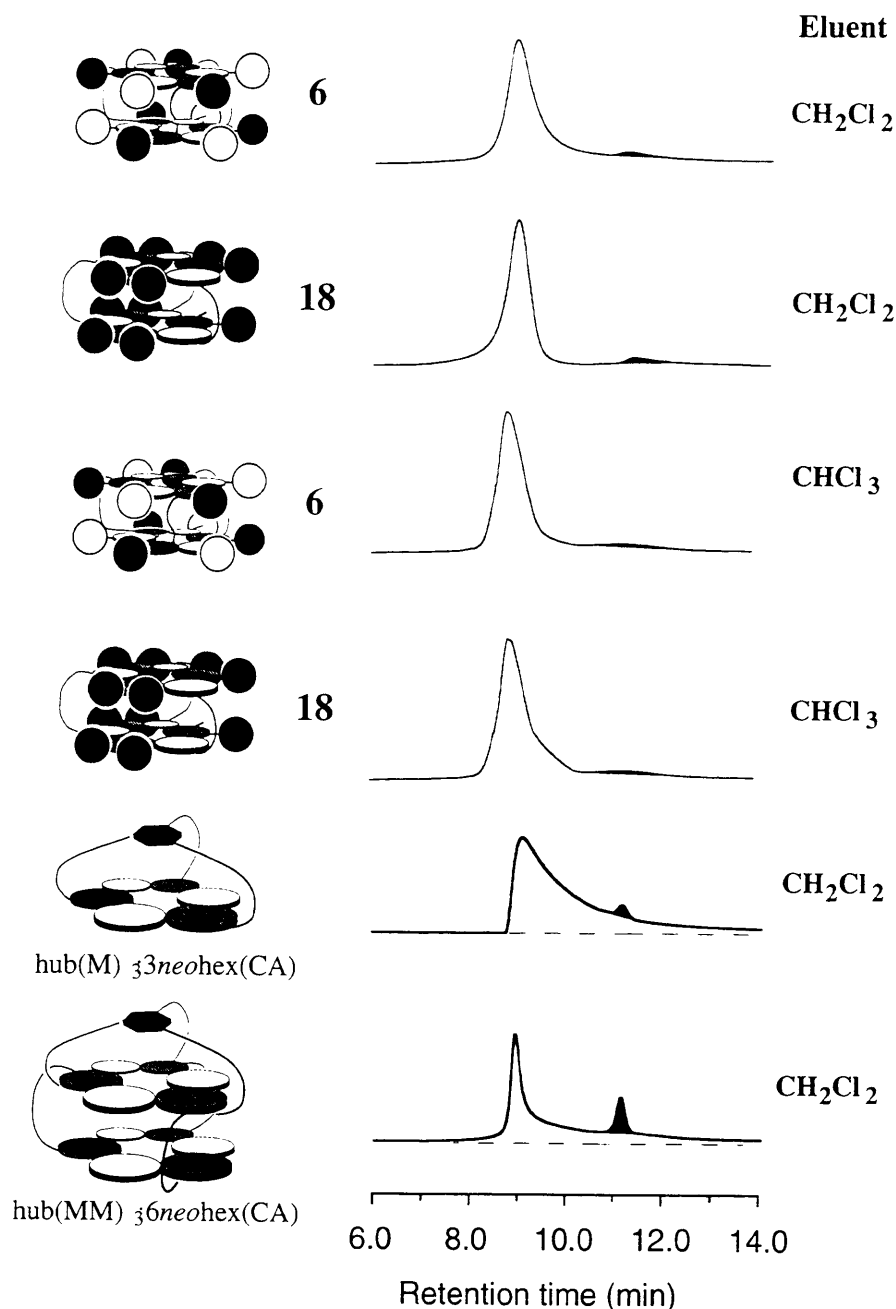
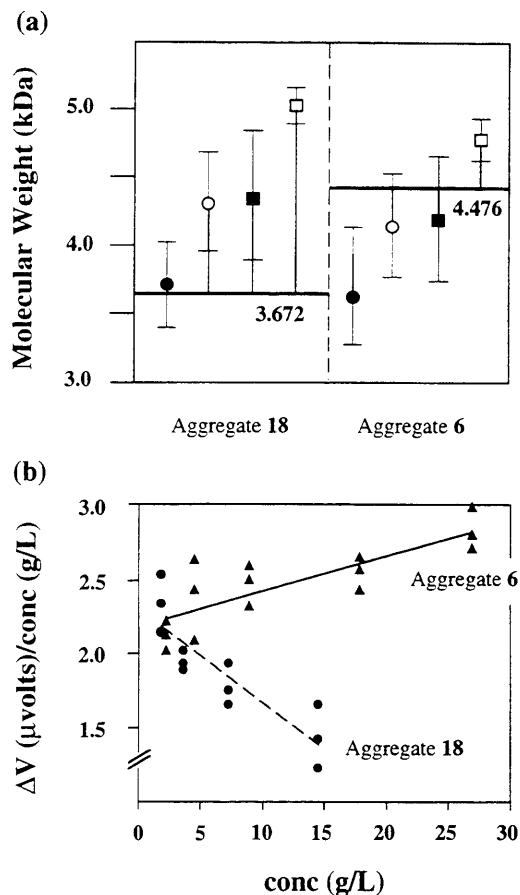


Figure 7. Traces from GPC for the aggregates **6** and **18** with chloroform and methylene chloride as the eluent. Traces for two self-assembled aggregates based on covalent preorganization, hub(M)<sub>3</sub>:3neo<sub>6</sub>hex(CA) and hub(MM)<sub>3</sub>:6neo<sub>6</sub>hex(CA), are included for comparison of the peak shapes and retention times. Methylene chloride was the eluent in these cases, and *p*-xylene (darkened) was included as an internal reference. (The difference in the widths of the peak due to *p*-xylene is due to the aging of the column.) The lack of tailing for **6** and **18** is not a reflection on relative stability but rather on the insolubility of these aggregates upon the loss of one or more components. The hub aggregates are significantly more soluble upon loss of one or more molecules of CA.

The change from **4** (R' = 'Bu) to **7** (R' = H) reduces the steric bulk associated with the melamines. This feature should,

therefore, reduce the extent of peripheral crowding involved in the association of these components with isocyanurates. We



**Figure 8.** (a) Estimation of the molecular weights in solution by vapor pressure osmometry of the aggregates **6** and **18**. Calculated molecular weights for each aggregate are given in each column by solid horizontal bars and the associated numbers. In each case, measurements were made against four different standards: *N,N'*-bis-*t*-Boc-gramicidin S (MW 1342) (•), sucrose octaacetate (MW 679) (○), polystyrene (av MW 5050, polydispersity 1.05) (■), and perbenzoyl- $\beta$ -cyclodextrin (MW 3321) (□). Error bars represent standard deviations of measurements on aggregate and standards. Measurements were made in chloroform at 233 K with concentrations in the range 0.5–6 mM. (b) Plot of  $\Delta V$ /conc vs conc showing the difference in the concentration-dependence of data from VPO for **6** and **18** ( $\Delta V$  is the change in voltage required to maintain the thermistor at constant temperature). Lines represent least-squares analysis of these data.

expect, therefore, that the driving force selecting for the formation of the  $CA_3M_3$  rosette over competing linear hydrogen-bonded networks would be lower in **7** than in **4**. Both **4** and **7** form stable aggregates of composition  $3bis(M)_2:6Ph_3Pr(CA)$  on mixing with **5** (Table 1). As the steric requirement of the isocyanurate was reduced ( $35 < 34 < 1 < 5$ ), however, the effects on the self-assembly of  $CA_3M_3$  rosettes become apparent with **7** before **4**. For example, while **4** forms a stable aggregate on mixing with *neohexylisocyanurate* **34**, **7** does not. These observations indicate that reducing the steric bulk of the substituents on the melamines and those on the isocyanurates and barbiturates decreases the stability of aggregates based on  $CA_3M_3$  rosettes. The proclivity of the bulky isocyanurate **5** to form aggregates based on connected  $CA_3M_3$  rosettes, even in the absence of sterically demanding substituents on the melamines, reinforces the suggestion—indicated by studies on aggregates comprising a single  $CA_3M_3$  rosette<sup>7</sup>—that this particular isocyanurate provides a strong driving force selecting for the self-assembly of  $CA_3M_3$  rosettes. These data demonstrate the importance of the size of the substituent R on the melamines in biasing self-assembly in favor of aggregates based on  $CA_3M_3$  rosettes.

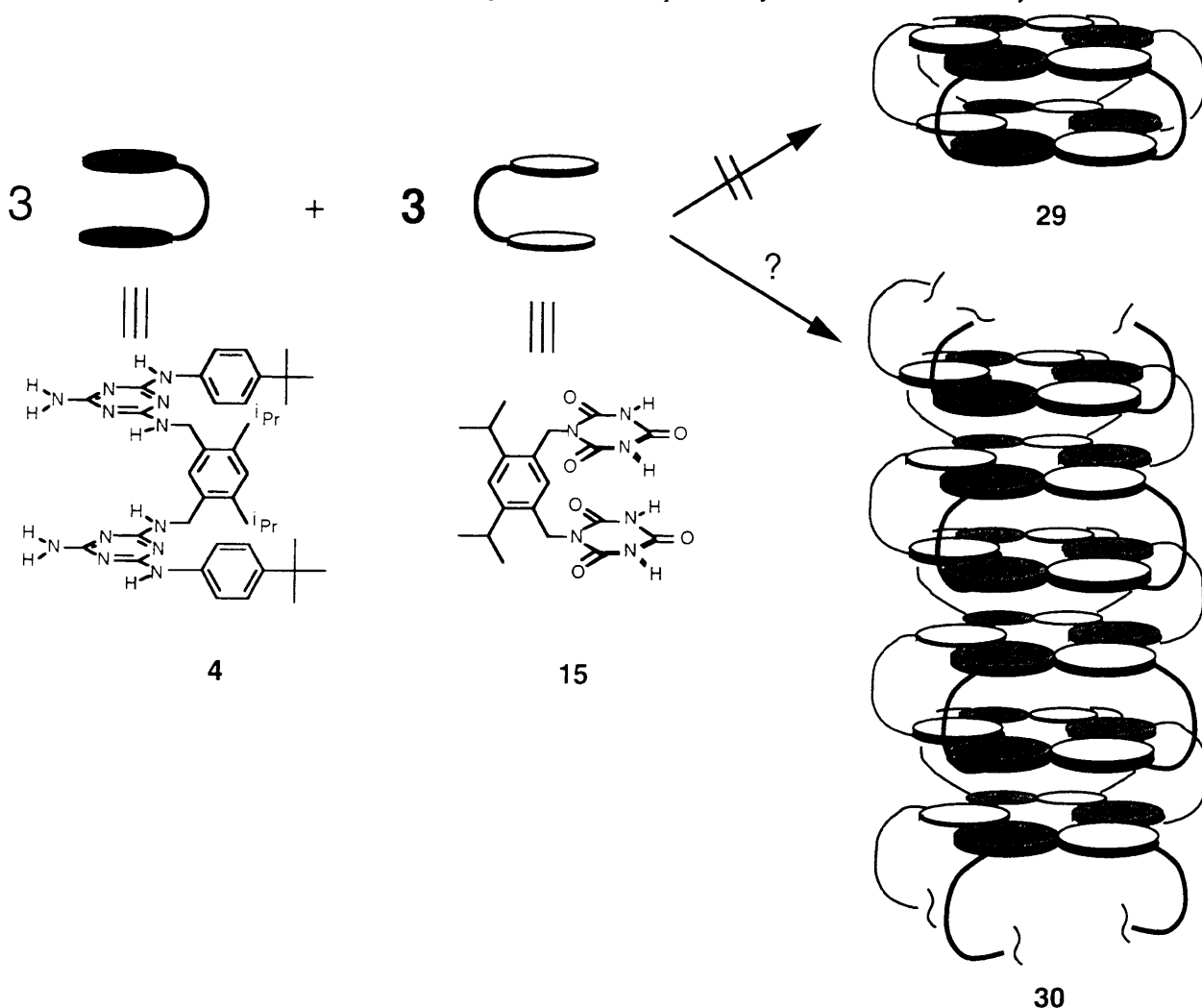
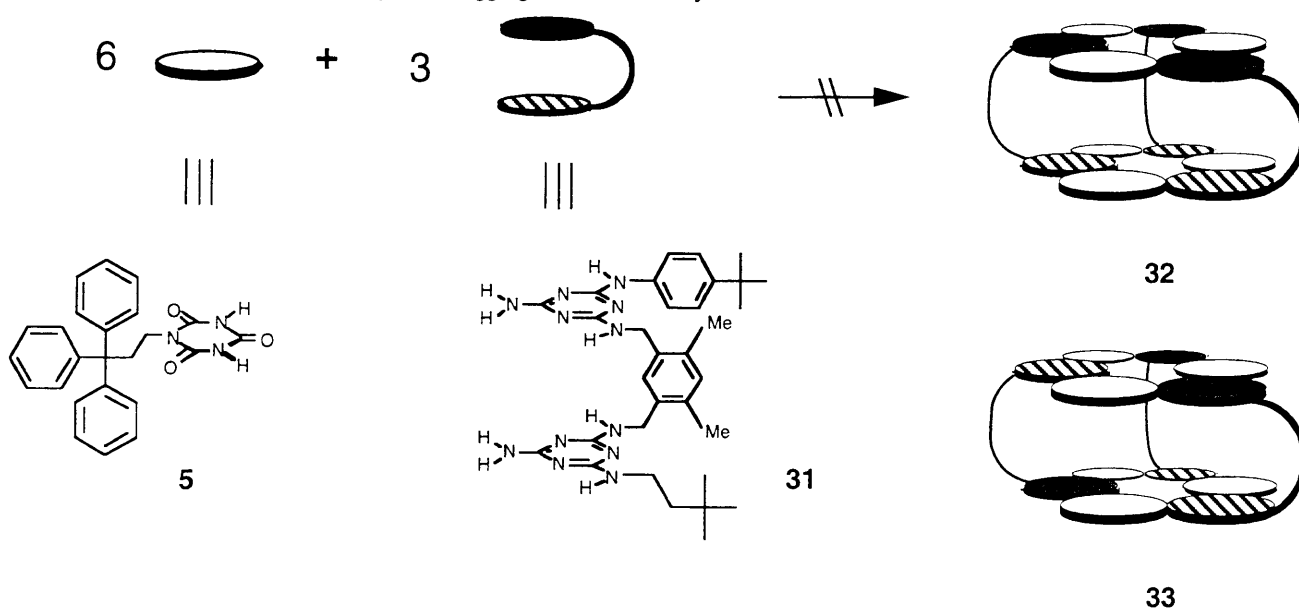
We have also used a second level of steric hindrance to assist/select for the self-assembly of these aggregates. The isopropyl

substituents on the *m*-xylyl linker in the bismelamine **4** inhibit rotation about the bonds linking the melamines to the linker and, therefore, hold them preorganized in the geometry required for formation of the bisrosette. We prepared the three bismelamines **4** (R = *i*Pr), **8** (R = Me), and **9** (R = H), to examine the effects of altering the degree of preorganization on the self-assembly of  $CA_3M$  rosettes (Table 1). We expected that reducing the size of the substituent R would reduce the degree to which the geometry of the two melamines in the uncomplexed state matches that in the aggregate and, therefore, reduce the ability of the components to assemble successfully into bisrosettes. Again, mixing 3 equiv of the bismelamines **4**, **8**, and **9** with 6 equiv of the bulky isocyanurate **5** affords a self-assembled aggregate of composition  $3bis(M)_2:6Ph(CA)_3$  (Table 1). The stability of these aggregates as discrete structural entities over time (96 h), however, appears to differ, as judged by their tendency to precipitate.

Precipitation occurs from solutions of the aggregates formed between  $Ph_3Pr(CA)$  **5** and the bismelamines **8** or **9** on standing. The suspensions formed over time in these cases can be solubilized by adding methanol and additional chloroform, concentrating in vacuo, and redissolving in chloroform alone. Spectra of these solutions from <sup>1</sup>H NMR show that the aggregates have reassembled, before precipitation occurs once again. Precipitation (from the initially homogeneous solution) occurs in the order **9** (much precipitation) > **8** (slight precipitation) > **4** (no precipitation). We note that precipitation (**9** > **8** > **4**) from these aggregates correlates with the reduction in preorganization (**4** > **8** > **9**). The progressive reduction in preorganization from **4** through **8** to **9** correlates with the failure of the components to self-assemble and afford thermodynamically stable aggregates based on connected  $CA_3M_3$  rosettes. Three plausible explanations for this precipitation are (i) the aggregate is dissociating into its constituent molecules, which are then precipitating from solution, (ii) the aggregate is dissociating slowly and the free components reassociating into a random hydrogen-bonded oligo/polymer, or (iii) the aggregate is associating into larger assemblies. The correlation between the preorganization of the components and the degree of precipitation suggests that either (i) or (ii) is the most likely cause of precipitation. As preorganization is related, the discrete aggregate appears to become a metastable state (the kinetic product of self-assembly), rather than a thermodynamically stable hydrogen-bonded state.

The bismelamine **10** (R' = Me, R = H) demonstrates the effect of reducing both the steric bulk of the substituents on the melamines and the preorganization of the two melamines for self-assembly. This component is the least successful at forming aggregates of composition  $3bis(M)_2:6(CA)$  on mixing with 6 equiv of isocyanurates or barbiturates. This result supports the conclusions that both steric bulk at the periphery of the aggregate and preorganization of the components play a significant role in selecting for/directing the self-assembly of  $CA_3M_3$  rosettes.

Mixing 3 equiv of the bisisocyanurate, **15** or **16**, with 6 equiv of the melamine derivatives **36–38** that are substituted by groups smaller than *p*-*tert*-butylphenyl (as in **2**) does not afford well-defined bisrosettes (Table 2). Homogenous solutions of the components in  $CHCl_3$  are not obtained on mixing the molecules in chloroform, even after sonication and heating. <sup>1</sup>H NMR spectroscopy on the soluble portions of these mixtures do not reveal the presence of any well-defined aggregates. The steric bulk of the two *p*-*tert*-butylphenyl groups appears, therefore, to be responsible for selecting for the formation of the  $CA_3M_3$  rosettes in these cases. Reducing the steric bulk of the substituents on the melamines decreases the stability of  $CA_3M_3$  rosettes. This observation correlates strongly with those made on aggregates comprising a single  $CA_3M_3$  rosette in the previous paper. The self-assembly of  $CA_3M_3$  rosettes between barbitol (**1**) and *N,N'*-substituted phenylmelamines was equally sensitive to the steric bulk of the substituent of the phenyl rings. Derivatives of

**Scheme 7.** Attempted Self-Assembly of an Aggregate between Complementary Bismelamine and Bisisocyanurate Derivatives**Scheme 8.** Attempted Self-Assembly of an Aggregate from an Unsymmetrical Bismelamine Derivative

melamine bearing two phenyl, adamantyl (37), or *p*-tolyl (38) substituents did not form  $CA_3 \cdot M_3$  rosettes with barbital.

*Isocyanurate protons are useful structural markers in the characterization of self-assembled aggregates based on  $CA_3 \cdot M_3$  rosettes.* The full characterization of these self-assembled

aggregates by  $^1H$  NMR spectroscopy is important. We have found the region between  $\delta$  13 and 17 ppm in the  $^1H$  NMR spectrum particularly useful in assessing the fundamental structural features of new supramolecular aggregates based on  $CA_3 \cdot M_3$  rosettes; other regions of the NMR spectrum can be

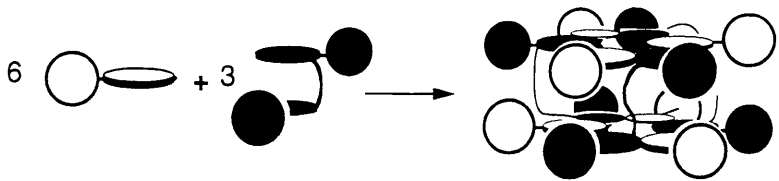
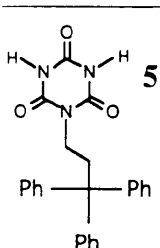
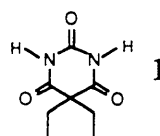
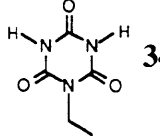
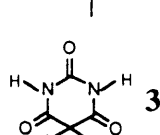
**Table 1.** Outcome of Self-Assembly of Various Bismelamine Derivatives, **4** and **7–10**, with Different Isocyanurates and Barbiturates<sup>a</sup>


Diagram illustrating the self-assembly of bismelamine derivatives (**4** and **7–10**) with different isocyanurates (**5**, **1**, **34**, **35**). The diagram shows the reaction of 6 molecules of a bismelamine derivative with 3 molecules of an isocyanurate to form a complex aggregate. The bismelamine derivative has a central benzene ring with two R groups and two NH groups, each connected to a melamine ring. The isocyanurate has a central carbon atom bonded to three nitrogen atoms, each with a hydrogen atom. The aggregate is a complex, three-dimensional structure.

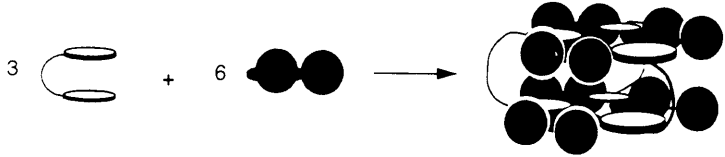
	increasing steric bulk of R'		increasing preorganization (size of R)		
	<b>7</b> R' = H R = <i>i</i> Pr	<b>4</b> R' = <i>t</i> Bu R = <i>i</i> Pr	<b>8</b> R' = <i>t</i> Bu R = Me	<b>9</b> R' = <i>t</i> Bu R = H	<b>10</b> R' = Me R = H
<b>5</b> 	++	++	++	+	+
<b>1</b> 	++	++	+	+	-
<b>34</b> 	-	++	-	-	-
<b>35</b> 	-	+	-	-	-

<sup>a</sup> ++ Indicates successful formation of a stable aggregate. + Indicates formation of the aggregate as a homogeneous solution in chloroform from which precipitation occurs over 24–96 h. - Indicates that a well-defined aggregate is not formed on mixing the components.

complicated by overlap of different resonances. This low-field region of the spectrum contains only the resonances of the hydrogen-bonded protons on the isocyanurates (Figure 9). Overlap between different types of protons is, therefore, not a problem. Furthermore, the isocyanurate protons are involved directly in the hydrogen-bonded CA<sub>3</sub>·M<sub>3</sub> rosette; their resonances are, therefore, sensitive to the degree of hydrogen bonding, concentration, temperature, environment, symmetry of the hydrogen-bonded network, and exchange between associated and dissociated states. In summary, the resonances from these protons provide a wealth of information about the global and local structure of new self-assembled aggregates.

The utility of these resonances in the characterization of aggregates has been demonstrated by the assignment of the relationships between adjacent CA<sub>3</sub>·M<sub>3</sub> rosettes in **6** and **18**. The resonances of the isocyanurate protons from these aggregates are shown in Figure 9b,c, respectively. Once the symmetry of the hydrogen-bonded network has been ascertained, the complete assignment of the resonances to the aggregates can be relatively straightforward.

The complexity of the region in the <sup>1</sup>H NMR spectrum between δ 13 and 17 ppm in Figure 9a mirrors the irregularity of the aggregates formed on mixing **4** and **15** (Scheme 7). This complexity is not consistent with the formation of the desired

**Table 2.** Outcome of Self-Assembly of Two Bisisocyanurate Derivatives, **15** and **16**, with Different Melamine Derivatives<sup>a</sup>


	<b>2</b>	<b>36</b>	<b>37</b>	<b>38</b>
<b>15</b>	++	-	-	-
<b>16</b>	++	-	-	-

<sup>a</sup> ++ Indicates successful formation of a stable aggregate. - Indicates that a well-defined aggregate is not formed on mixing the components. The relative size of the substituents on **37** (compared with others in the series) is unclear. The adamantyl groups may be too large.

single aggregates **29** and **32**. The aggregate formed on mixing 3 equiv of the bismelamine **4** with 6 equiv of *neohexylisocyanurate* **34** in chloroform provides another example of the information provided by the resonances of the isocyanurate protons. This aggregate displays four resonances (the middle resonance is the superposition of two singlets) for the isocyanurate protons (Figure 9d). It has a structure, therefore, in which both  $CA_3 \cdot M_3$  rosettes display two resonances for the isocyanurate protons, and the two rosettes, themselves, are not related by a mirror plane of symmetry or by rotation through  $180^\circ$  about an axis parallel to that of the isocyanurates. This feature contrasts to the aggregate **6** formed between **4** and **5** in which the two adjacent rosettes are related by such symmetry. Variable-temperature  $^1H$  NMR spectroscopy is consistent with the hypothesis that all four resonances in the aggregate between **4** and **34** are derived from a *single* conformation of a *single* aggregate (Figure 9d,e). No changes in relative proportion (by integration), chemical shift, peak shape, or number of peaks occur on cooling the sample from 298 to 233 K that would indicate any exchange between conformations or associated/dissociated states is occurring. Although the gross structures (*i.e.*, composition) of the aggregate formed between **4** and **5** or **34** are the same— $3bis(M)_2:6R(CA)$ —the reduction in steric demand on the change from **5** to **34** is accompanied by changes in the local structure of the aggregate. This feature indicates,

once again, that steric interactions at the periphery of the aggregates do play a significant role in determining the outcome of the association between these components.

Aggregates based on two connected  $CA_3 \cdot M_3$  rosettes are more stable than those based on a single  $CA_3 \cdot M_3$  rosette. Both  $^1H$  NMR spectroscopy and gel permeation chromatography indicate that aggregates comprising two connected  $CA_3 \cdot M_3$  rosettes and showing peripheral crowding are more stable than those based on a single  $CA_3 \cdot M_3$  rosette. The presence of resonances for the fully assembled aggregate of composition  $3bis(M)_2:6Ph_3Pr(CA)$  in the  $^1H$  NMR spectrum before addition of a full 2 equiv of  $Ph_3Pr(CA)$  to  $bis(M)_2$  (Scheme 3) alongside those of uncomplexed components and intermediates along the assembly pathway (see Figure 3) indicates that the rates of interchange of bisrosettes is slower than those for aggregate comprising a single  $CA_3 \cdot M_3$  rosette. The absence of concentration-dependent dissociation of **6** and **18** on dilution of their solutions reinforces this conclusion. The observation of peaks for the aggregates **6** and **18** in GPC that are relatively sharp also suggests that the stability of these bisrosettes is greater than that of aggregates based on a single  $CA_3 \cdot M_3$  rosette.

These observations correlate with those made on aggregates that comprise increasing numbers of parallel, connected  $CA_3 \cdot M_3$  rosettes in the series based on covalent preorganization, such as

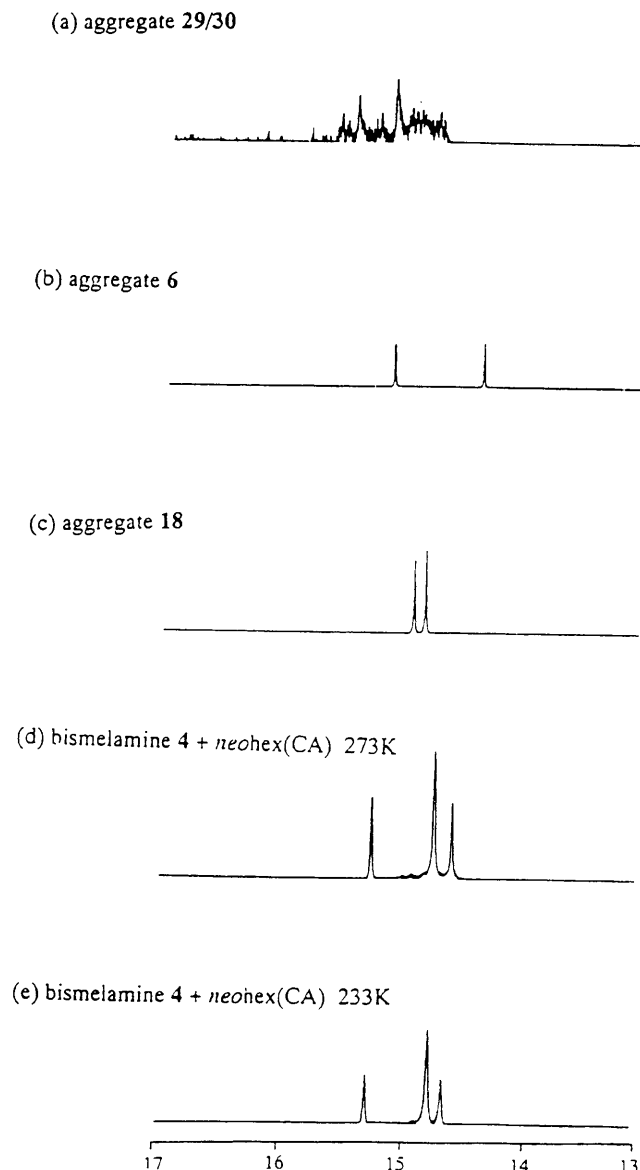


**Figure 9.** Portions of the  $^1\text{H}$  NMR spectra of the self-assembled aggregates showing the resonances associated with the hydrogen-bonded isocyanurate protons ( $\text{CDCl}_3$ , 500 MHz).

hub(M) $_3$ :3neohex(CA) and hub(MM) $_3$ :6neohex(CA) shown in Figure 1. In this case, the latter is more stable than the former.<sup>8</sup> In both of the series—one based on peripheral crowding and the other based on covalent preorganization of melamines—we believe that the increase in stability of the aggregates based on parallel  $\text{CA}_3\cdot\text{M}_3$  rosettes relative to those based on single  $\text{CA}_3\cdot\text{M}_3$  rosette is a consequence of the extra preorganization imparted to each  $\text{CA}_3\cdot\text{M}_3$  rosette by the neighboring  $\text{CA}_3\cdot\text{M}_3$  rosette. It is also reflected in the ratio of hydrogen bonds stabilizing the aggregate (enthalpy) to the number of particles involved in the aggregate (entropy).

## Conclusions

Supramolecular aggregates based on two connected  $\text{CA}_3\cdot\text{M}_3$  rosettes—bisrosettes **6** and **18**—are more stable than aggregates based on single  $\text{CA}_3\cdot\text{M}_3$  rosette **3**. Indeed, bisrosettes based on connected  $\text{CA}_3\cdot\text{M}_3$  units obtained by peripheral crowding display a surprisingly high degree of stability. The structures described in this paper illustrate that 36 hydrogen bonds can stabilize supramolecular aggregates composed of nine particles. The ability to prepare stable self-assembled aggregates by peripheral crowding renders this strategy a useful addition to that based on covalent

preorganization for the formation of supramolecular aggregates stabilized by  $\text{CA}_3\cdot\text{M}_3$  rosettes.

The “rules/observations” that were inferred to govern the assembly of aggregates comprising a single  $\text{CA}_3\cdot\text{M}_3$  rosette<sup>7</sup> by peripheral crowding are paralleled by those for the aggregates based on connected  $\text{CA}_3\cdot\text{M}_3$  rosettes. Most importantly, the stability of  $\text{CA}_3\cdot\text{M}_3$  rosettes does decrease as the size of the substituents on the melamines and isocyanurates is reduced.

## Experimental Section

**General Methods.** NMR experiments were performed with a Bruker AM 500 or 400 instrument. THF was distilled from sodium benzophenone ketyl. Methylene chloride and triethylamine were distilled from calcium hydride. Dimethylformamide was dried and stored over 4 Å molecular sieves. The compounds that have a triazine unit in their chemical structures show doubling of several resonances in their  $^1\text{H}$  and  $^{13}\text{C}$  NMR spectra due to slow exchange of conformers around the NHR–triazine bonds. Reagents were purchased from Aldrich–Sigma and were used without further purification. Abbreviations are used as follows: trifluoroacetic acid (TFA), diisopropylethylamine (DIPEA). Ammonium hydroxide ( $\text{NH}_4\text{OH}$ ) was used as a 30% aqueous solution.

**NOE Spectra.** The NOE spectra of these supramolecular aggregates were recorded at 25 °C, with an evolution period of 3.0 s and a relaxation delay of 6.0 s. The complex (5.0  $\mu\text{mol}$ ) was dissolved in 0.7 mL of  $\text{CDCl}_3$ , and the samples were degassed with five freeze–pump–thaw cycles.

**Gel Permeation Chromatography.** Gel permeation chromatography was performed using a Waters 600E HPLC with a Waters 484 UV detector and Waters analytical gel permeation column (Ultrastragel, 1000 Å pore size). Elutions were performed at room temperature using HPLC grade  $\text{CH}_2\text{Cl}_2$  or  $\text{CHCl}_3$  (containing 3.0 mM *p*-xylene as an internal reference) as the eluent at a flow rate of 1.0 mL/min. The samples were prepared at concentrations of the complexes of 1 mM. The injection volume was 20  $\mu\text{L}$ .

**Molecular Weight Determinations by Vapor Pressure Osmometry.** Molecular weight determinations were made with a Wescan Model 233 vapor pressure osmometer operated at 35 °C. The molecular weight of the complexes were measured in HPLC grade, glass-distilled chloroform at concentrations of approximately 0.5, 1, 2, 4, and 6 mM. At each concentration, 3–5 measurements were taken. Calibration curves were generated using four molecular weight standards: sucrose octaacetate (MW 679), perbenzoyl  $\beta$ -cyclodextrin (MW 3321), polystyrene (MW 5050, polydispersity = 1.05), and a derivative of gramicidin S in which the two ornithine amino groups had been converted to their *tert*-butylcarbamates (MW 1342).<sup>2</sup>

**Carbamic Acid, [[5-[[[4-Amino-6-[[4-(1,1-dimethylethyl)phenyl]amino]-1,3,5-triazin-2-yl]amino]methyl]-2,4-bis(1-methylethyl)phenyl]methyl]-1,1-dimethylethyl Ester (24).** A 100-mL, three-necked, round-bottomed flask was charged with cyanuric chloride (362 mg, 1.96 mmol), THF (30 mL), and DIPEA (1 mL), and the solution was cooled to 0 °C under an atmosphere of nitrogen. To the solution was added *p*-*tert*-butylaniline (0.31 mL, 0.29 mg, 1.96 mmol) in three portions over 10 min. After 1 h, the reaction mixture was warmed to room temperature, and the amine **22** (629 mg, 1.96 mmol)<sup>2</sup> was added. This mixture was stirred at 30 °C for 2 h. The reaction mixture was cooled to room temperature and concentrated in vacuo. The residue was partitioned between EtOAc (125 mL) and brine (75 mL). The organic extract was washed with further brine (75 mL), dried over  $\text{MgSO}_4$ , filtered, and concentrated in vacuo to afford the monochloro triazine **23**. This material was dissolved in 1,4-dioxane (11 mL) and 30% aqueous  $\text{NH}_4\text{OH}$  (7 mL). The solution was sealed in a Parr vessel and heated at 95 °C for 8 h. The mixture was cooled to room temperature, depressurized, and concentrated in vacuo. The residue was partitioned between EtOAc (175 mL) and brine (125 mL). The organic extract was washed with further brine (100 mL), dried over  $\text{MgSO}_4$ , filtered, and concentrated in vacuo. The residue was purified by column chromatography on silica gel using a solution of  $\text{NH}_4\text{OH}/\text{MeOH}$  (1/19 v/v) in  $\text{CH}_2\text{Cl}_2$  (1/19 v/v) to afford the product as a white crystalline material (868 mg, 1.54 mmol, 86%):  $^1\text{H}$  NMR (500 MHz,  $\text{DMSO}-d_6$ )  $\delta$  8.68 (br app d, 1 H), 7.61 (br s, 1 H), 7.54 (br s, 1 H), 7.30–7.10 (br m, 6 H), 6.30–6.10 (br app d, 2 H), 4.50–4.40 (br app d, 2 H), 4.09 (br s, 2 H), 3.20–3.10 (2  $\times$  m, 2  $\times$  1 H), 1.35 (s, 9 H), 1.22 (s, 9 H), and 1.15 (m, 12 H);  $^{13}\text{C}$  NMR (125 MHz,  $\text{DMSO}-d_6$ )  $\delta$  164.39, 144.55, 133.32, 124.65, 121.29, 119.40, 77.55, 40.91, 33.75,

31.22, 28.21, 27.74, 37.67, and 23.74; HRMS-FAB ( $M + H$ )<sup>+</sup> calcd for  $C_{32}H_{48}N_7O_2$  562.3869, found 562.3868.

***N,N'*'-[[4,6-Bis(1-methylethyl)-1,3-phenylene]bis(methylene)]bis[*N'*-(4-(1,1-dimethylethyl)phenyl)]-1,3,5-triazine-2,4,6-triamine (4).** A solution of **9** (800 mg, 1.43 mmol) in  $CH_2Cl_2$  (50 mL) was cooled to 0 °C. TFA (4 mL) was added dropwise over 10 min, and the mixture was stirred for 2 h, under an atmosphere of nitrogen. The reaction mixture was diluted with toluene (50 mL) and concentrated in vacuo. The residue was partitioned between EtOAc (100 mL) and 1 N NaOH (75 mL). The organic extract was washed with brine (2 × 50 mL), dried over  $MgSO_4$ , filtered, and concentrated in vacuo to unprotected amine. This material was added to a solution of **21** (424 mg, 1.43 mmol) (prepared *in situ*) in THF (100 mL) and DIPEA (10 mL), and the solution was stirred at 30 °C for 5 h. The reaction mixture was cooled to room temperature and concentrated in vacuo. The residue was dissolved in 1,4-dioxane (15 mL) and 30% aqueous  $NH_4OH$  (10 mL). The solution was sealed in a Parr vessel and heated at 105 °C for 12 h. The mixture was cooled to room temperature, depressurized, and concentrated in vacuo. The residue was partitioned between EtOAc (300 mL) and brine (200 mL). The organic extract was washed with further brine (200 mL), dried over  $MgSO_4$ , filtered, and concentrated in vacuo. The residue was purified by column chromatography on silica gel using a solution of  $NH_4OH$ /MeOH (1/9:v/v) in  $CH_2Cl_2$  (1/19:v/v) to afford the product as a white crystalline material (612 mg, 0.87 mmol, 61%):  $^1H$  NMR (500 MHz,  $DMSO-d_6$ )  $\delta$  8.75–8.62 (br m, 2 H), 7.61–7.52 (br m, 2 H), 7.25–7.05 (br m, 10 H), 6.30–6.13 (br m, 4 H), 4.49–4.40 (br m, 4 H), 3.22–3.15 (br m, 2 H), and 1.28–1.10 (br m, 30 H);  $^{13}C$  NMR (125 MHz,  $DMSO-d_6$ )  $\delta$  166.65, 165.83, 143.51, 137.86, 125.44, 124.83, 121.49, 119.60, 113.84, 33.91, 33.89, 31.57, 31.33, 27.94, and 23.84; HRMS-FAB ( $M + H$ )<sup>+</sup> calcd for  $C_{40}H_{55}N_{12}$  703.4672, found 703.4689.

***N,N,N',N'*'-[[4,6-Bis(1-methylethyl)-1,3-phenylene]bis(methylene)]bis[*N'*-(4-phenyl)]-1,3,5-triazine-2,4,6-triamine (7).** A 100-mL, three-necked, round-bottomed flask was charged with cyanuric chloride (303 mg, 1.65 mmol), THF (20 mL), and DIPEA (1.5 mL), and the solution was cooled to 0 °C under an atmosphere of nitrogen. Aniline (**25**) (0.15 mL, 1.65 mmol) was added to the solution in two portions over 5 min. After 45 min the reaction mixture was warmed to room temperature, and the bisamine **27** (182 mg, 0.825 mmol)<sup>3</sup> was added. This mixture was stirred at 25 °C for 6 h. The reaction mixture was cooled to room temperature and concentrated in vacuo. This material was dissolved in 1,4-dioxane (13 mL) and 30% aqueous  $NH_4OH$  (9 mL). The solution was sealed in a Parr vessel and heated at 115 °C for 28 h. The mixture was cooled to room temperature, depressurized, and concentrated in vacuo. The residue was washed with cold water and filtered, and the solid residue was recrystallized from MeOH to afford the product as a cream solid (311 mg, 0.528 mmol, 64%):  $^1H$  NMR (500 MHz,  $DMSO-d_6$ )  $\delta$  8.98–8.74 (br m, 2 H), 7.78–7.64 (br m, 2 H), 7.21–6.81 (br m, 12 H), 6.37 (br s, 4 H), 4.50–4.38 (br m, 4 H), 3.24–3.15 (br s, 2 H), and 1.16 (br s, 12 H);  $^{13}C$  NMR (125 MHz,  $DMSO-d_6$ )  $\delta$  165.80, 164.12, 145.12, 133.08, 128.14, 121.44, 119.43, 116.08, 41.03, 27.86, and 26.73; HRMS-FAB ( $M + H$ )<sup>+</sup> calcd for  $C_{32}H_{39}N_{12}$  591.3420, found 591.3426.

***N,N,N',N'*'-[(4,6-Dimethyl-1,3-phenylene)bis(methylene)]bis[*N'*-(4-(1,1-dimethylethyl)phenyl)]-1,3,5-triazine-2,4,6-triamine (8).**  $^1H$  NMR (500 MHz,  $DMSO-d_6$ )  $\delta$  8.72–8.60 (br m, 2 H), 7.60–7.50 (br m, 3 H), 7.23–7.15 (br m, 4 H), 7.05–6.92 (br s, 3 H), 6.28–6.15 (br m, 4 H), 4.36 (br s, 4 H), 2.21 (s, 6 H), and 1.20 (s, 18 H);  $^{13}C$  NMR (125 MHz,  $DMSO-d_6$ )  $\delta$  167.10, 166.79, 165.97, 164.37, 145.41, 143.28, 137.84, 135.02, 131.42, 124.61, 124.58, 119.52, 119.41, 43.26, 33.66, 31.17, and 18.14; HRMS-FAB ( $M + H$ )<sup>+</sup> calcd for  $C_{36}H_{47}N_{12}$  647.4046, found 647.4040.

***N,N,N',N'*'-[1,3-Phenylenebis(methylene)]bis[*N'*-(4-(1,1-dimethylethyl)phenyl)]-1,3,5-triazine-2,4,6-triamine (9).**  $^1H$  NMR (500 MHz,  $DMSO-d_6$ )  $\delta$  8.77–8.65 (br m, 2 H), 7.65–7.52 (br m, 4 H), 7.30–7.11 (br m, 8 H), 6.36–6.15 (br m, 4 H), 4.47 (br s, 4 H), and 1.22 (s, 18 H);  $^{13}C$  NMR (125 MHz,  $DMSO-d_6$ )  $\delta$  166.83, 166.16, 164.43, 143.36, 140.40, 137.82, 127.84, 125.55, 125.14, 124.61, 119.55, 119.43, 43.20, 33.67, and 31.17; HRMS-FAB ( $M + H$ )<sup>+</sup> calcd for  $C_{34}H_{43}N_{12}$  619.3733, found 619.3748.

***N,N,N',N'*'-[1,3-Phenylenebis(methylene)]bis[*N'*-(4-methylphenyl)]-1,3,5-triazine-2,4,6-triamine (10).**  $^1H$  NMR (500 MHz,  $DMSO-d_6$ )  $\delta$  8.77–8.67 (br m, 2 H), 7.65–7.54 (br m, 4 H), 7.27–7.18 (br m, 4 H), 7.12 (br s, 2 H), 6.96 (br s, 2 H), 6.46–6.17 (br m, 4 H), 4.43 (b,  $J_{ab} = 6.8$  Hz, 4 H), and 2.19 (s, 6 H);  $^{13}C$  NMR (125 MHz,  $DMSO-d_6$ )  $\delta$  166.81, 166.15, 164.42, 140.51, 138.23, 129.77, 128.56, 127.91, 125.511, 119.52, 43.11, and 20.31; HRMS-FAB ( $M + H$ )<sup>+</sup> calcd for  $C_{28}H_{31}N_{12}$  535.2794, found 535.2789.

***N*'-[[5-[[4-Amino-6-[(3,3-dimethylbutyl)amino]-1,3,5-triazin-2-yl]amino]methyl]-2,4-bis(1-methylethyl)phenyl]methyl]-*N'*-(4-(1,1-dimethyl)phenyl)]-1,3,5-triazine-2,4,6-triamine (31).**  $^1H$  NMR (500 MHz,  $DMSO-d_6$ )  $\delta$  8.75–8.60 (br m, 2 H), 7.64–7.53 (br m, 2 H), 7.21–7.17 (br m, 4 H), 7.01–6.80 (br m, 2 H), 6.60–5.58 (br m, 4 H), 4.40–4.32 (br m, 4 H), 3.20–3.10 (br m, 2 H), 2.19 (s, 6 H), 1.41–1.32 (br m, 2 H), 1.22 (s, 9 H), and 0.95–0.78 (br s, 9 H);  $^{13}C$  NMR (125 MHz,  $DMSO-d_6$ )  $\delta$  166.77, 165.95, 165.64, 164.35, 145.16, 135.24, 133.42, 131.40, 124.59, 119.41, 42.86, 36.33, 33.67, 31.18, 29.41, 29.24, and 18.14; HRMS-FAB ( $M + H$ )<sup>+</sup> calcd for  $C_{32}H_{47}N_{12}$  599.4046, found 599.4036.

**Acknowledgment.** This work was supported by The National Science Foundation (Grants CHE-91-22331 to G.M.W. and DMR-89-20490 to the Harvard University Materials Research Laboratory). NMR instrumentation was supported by the National Science Foundation Grant CHE-88-14019 and the National Institutes of Health Grant 1 S10 RR4870. Mass spectrometry was performed by Dr. A. Tyler. The Harvard University Mass Spectrometry Facility was supported by The National Science Foundation Grant CHE-90-20043 and The National Institutes of Health Grant 1 S10 RR06716-01. We thank Professor Robert Cohen (MIT, Chemical Engineering) for the loan of his vapor pressure osmometer. J.P.M. was an SERC/NATO Postdoctoral Fellow, 1991–1993.